Inorg. Chem. **2004**, *43*, 2175–2182

Toward a Catalytic Cycle for the Mn–Salen Mediated Alkene Epoxidation: A Computational Approach

Luigi Cavallo and Heiko Jacobsen*,†

Department of Chemistry, Università di Salerno, Via Salvador Allende, Baronissi (SA) I-84081, Italy

Received November 24, 2003

BP86 density functional calculations for the title reaction are presented, where a model catalyst with hypochlorite as oxygen-containing counter ligand, (ClO)(O)Mn(acacen′) (acacen′ = $^{-}$O(CH)$_3$N–C$_2$H$_4$–N(CH)$_3$O^{-}), is employed. The epoxidation reaction on potential energy surfaces corresponding to an overall spin-density of two and four unpaired electrons is investigated. The presence of the hypochlorite ligand is found to cause the reaction to proceed under conservation of spin. Further, the oxygen-containing counter ligand causes reoxidation of the Mn-center, thus closing the catalytic cycle. A catalytic scheme is therefore proposed, which includes a step of regeneration of the catalytically active species. Energetic estimates including corrections for solvent effects are presented for the relevant steps constituting the proposed catalytic scheme.

1. Introduction

The enantioselective catalytic olefin epoxidation according to methodologies introduced and developed by Katsuki and Jacobsen has assumed a prominent role in the field of asymmetric catalysis over the past decade.[1] Jacobsen and co-workers reported for the first time the enantioselective epoxidation of olefins catalyzed by Mn−salen complexes in 1990.[2] Chiral Schiff base compounds such as **1a** were prepared and employed, following synthetic strategies previously developed by Kochi and co-workers.[3] Although iodosylmesitylene was used as an oxygen atom source, it was noted that sodium hypochlorite might also play the role of effective oxidant.[2] The use of undiluted commercial bleach under phase transfer conditions was suggested as a synthetic protocol, which was subsequently carefully reworked.[4] Efforts aimed at manipulating the ligand geometry needed to achieve ideal enantiomeric excess led to the synthesis of complex **1b**, which would later become known as "Jacobsen's catalyst" (Chart 1).

Chart 1

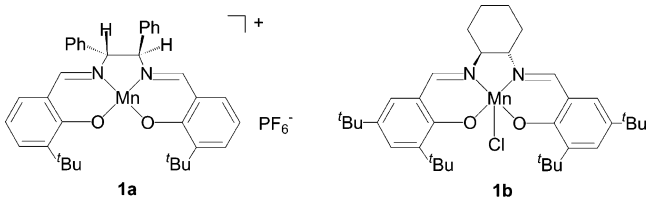

Complex **1b** is considered an effective catalyst for a large number of unfunctionalized olefins. Its facile method of preparation allows for industrial, ton scale production of the catalyst.[6] This very advantage has also led to the inclusion of the study of the Mn−salen catalyzed enantioselective epoxidation into chemistry curricula at universities and colleges.[7]

Concurrently, in 1990, Katsuki and co-workers reported the catalytic asymmetric epoxidation of unfunctionalized olefins using a different, chiral Mn−salen complex,[8] and to this day, the Jacobsen−Katsuki epoxidation has claimed a prominent role among the arsenal of chiral transformations available to the organic chemist.[9−15] Recent developments

* To whom correspondence should be addressed. E-mail: jacobsen@kemkom.com.

† Current address: KemKom, 15 Gwynne Avenue, Ottawa, Ontario, K1Y 1X1 Canada. Fax: (613) 729-2789.

(1) *Comprehensive Asymmetric Catalysis*; Jacobsen, E. N., Pfaltz, A., Yamamoto, H., Eds.; Springer: New York, 2000.
(2) Zhang, W.; Loebach, J. L.; Wilson, S. R.; Jacobsen, E. N. *J. Am. Chem. Soc.* **1990**, *112*, 2801.
(3) Srinivasan, K.; Michaud, P.; Kochi, J. K. *J. Am. Chem. Soc.* **1986**, *108*, 2309.
(4) Zhang, W.; Jacobsen, E. N. *J. Org. Chem.* **1991**, *56*, 2296.
(5) Jacobsen, E. N.; Zhang, W.; Muci, A. R.; Ecker, J. R.; Deng, L. *J. Am. Chem. Soc.* **1991**, *113*, 7063.
(6) Larrow, J. F.; Jacobsen, E. N.; Gao, Y.; Hong, Y. P.; Nie, X. Y.; Zepp, C. M. *J. Org. Chem.* **1994**, *59*, 1939.
(7) Hanson, J. *J. Chem. Educ.* **2001**, *78*, 1266.
(8) Irie, R.; Noda, K.; Ito, Y.; Matsumoto, N.; Katsuki, T. *Tetrahedron Lett.* **1990**, *31*, 7345.
(9) Jacobsen, E. N. In *Catalytic Asymmetric Synthesis*; Ojima, I., Ed.; VCH: Weinheim, 1993; Chapter 4.2.

10.1021/ic0353615 CCC: $27.50
Published on Web 02/27/2004

Scheme 1

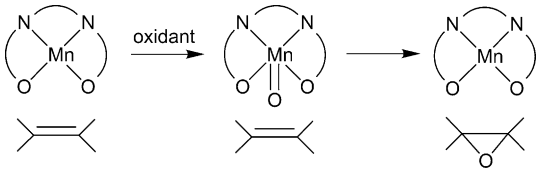

in the catalytic epoxidation with Mn−salen complexes include the use of ionic liquids,[16] which allow immobilizing, recovering, and recycling of the homogeneous chiral catalyst, and thus enhance the activity of the system. Lately, it has been reported that the use of ionic liquids extends the scope of the Jacobsen−Katsuki epoxidation to include molecular oxygen in the group of possible oxidizing agents.[17] Other ongoing research activities are concerned with the aspect of phase transfer. Salen ligand systems with built-in phase transfer capability have been designed, resulting in the formation of efficient catalysts for sodium hypochlorite epoxidation under biphasic reaction conditions.[18,19]

Given the importance of the Jacobsen−Katsuki epoxidation, it does not come as a surprise that over the last five years numerous density functional (DF) studies dealing with various aspects of the manganese mediated chiral epoxidation have appeared in the literature.[20−29,51] A theme of major interest is the mechanistic nature of this transformation. The most widely proposed scheme for the oxygen transfer reaction consists of a two-step catalytic cycle (Scheme 1). Here, oxygen is transferred from a terminal oxidant to a Mn(III)−salen catalyst, generating an intermediate Mn(V)−oxo complex, which in turn carries the activated oxygen to the olefinic double bond.[10,11,13]

The existence of a Mn(V)−oxo intermediate, first postulated by Kochi and co-workers,[3] was later proven by the utilization of electrospray tandem mass spectrometry techniques.[30] The highly debated second step of this reaction scheme,[31] the oxygen transfer from the transition metal center

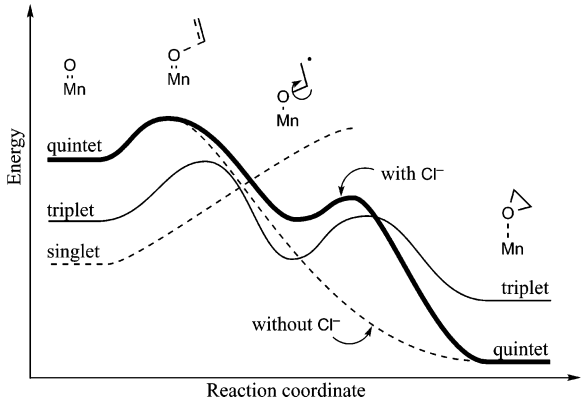

Figure 1. Qualitative consensus PES for the reaction of Mn−salen species with alkene. (Reprinted with permission from ref 32. Copyright 2002 Wiley-VCH.)

to the olefin, triggered the first DF studies devoted to the exploration of the potential energy surface (PES) on which the Jacobsen−Katsuki epoxidation occurs.[20,22] These studies were based on the cationic[20] and neutral[22] Mn−acacen′ model catalysts **2a** and **2b**, and the related oxo complexes **3a** and **3b** (acacen′ = $^{-}O(CH)_3N-C_2H_4-N(CH)_3O^{-}$), often employed in computations related to Mn−salen catalyzed epoxidation issues (Chart 2).

Chart 2

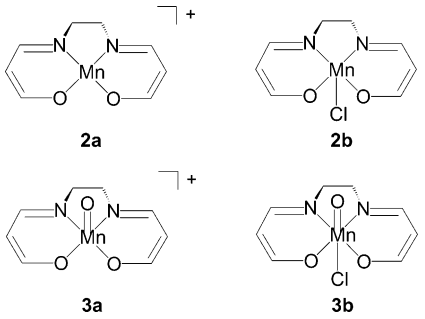

The resulting qualitative PES picture emerging from these early calculations[20,22] is depicted in Figure 1. Inspection of Figure 1 brings to light important issues commonly discussed in the context of the Jacobsen−Katsuki reaction mechanism. Two different catalytic systems are proposed, namely a neutral and a cationic species, respectively designated in Figure 1 as "with Cl^-", and "without Cl^-". For both types of catalysts, different spin systems are to be considered, including singlet, triplet, and quintet states. The reaction can then proceed in parallel on at least two different spin surfaces. The importance of spin-change and intersystem crossing for the course of the reaction as well as for its enantioselectivity has recently been discussed in the context of the related Cr−salen mediated epoxidation of alkenes, and the reader is referred to the literature for a detailed account of this subject.[32] A recent reinvestigation of the reaction scenario based on a cationic catalyst leads to the conclusion that the

(10) Jacobsen, E. N. In *Comprehensive Organometallic Chemistry II*; Wilkinson, G., Stone, F. G. A., Abel, E. W., Hegedus, L. S., Eds.; Pergamon: New York, 1995; Vol. 12, Chapter 11.1.
(11) Katsuki, T. *Coord. Chem. Rev.* **1995**, *140*, 189.
(12) Katsuki, T. *J. Mol. Catal. A: Chem.* **1996**, *113*, 87.
(13) Dalton, C. T.; Ryan, K. M.; Wall, V. M.; Bousquet, C.; Gilheany, D. G. *Top. Catal.* **1998**. *5*, 75.
(14) Flessner, T.; Doye, S. *J. Prakt. Chem.* **1999**, *341*, 436.
(15) Katsuki, T. *Adv. Synth. Catal.* **2002**, *344*, 131.
(16) Song, C. E.; Roh, E. J. *Chem. Commun.* **2000**, 837.
(17) Gaillon, L.; Bedioui, F. *Chem. Commun.* **2001**, 1458.
(18) Kureshy, R. I.; Khan, N. U. H.; Abdi, S. H. R.; Patel, S. T.; Iyer, P. K.; Jasra, R. V. *Tetrahedron Lett.* **2002**, *43*, 2665.
(19) Kureshy, R. I.; Khan, N. H.; Abdi, S. H. R.; Patel, S. T.; Iyer, P. K.; Subramanian, P. S.; Jasra, R. V. *J. Catal.* **2002**, *209*, 99.
(20) Linde, C.; Åkermark, B.; Norrby, P.-O.; Svensson, M. *J. Am. Chem. Soc.* **1999**, *121*, 5083.
(21) Strassner, T.; Houk, K. N. *Org. Lett.* **1999**, *1*, 419.
(22) Cavallo, L.; Jacobsen, H. *Angew. Chem.* **2000**, *112*, 602; *Angew. Chem., Int. Ed.* **2000**, *39*, 589.
(23) Jacobsen, H.; Cavallo, L. *Chem. Eur. J.* **2001**, *7*, 800.
(24) El-Bahraoui, J.; Wiest, O.; Feichtinger, D.; Plattner, D. A. *Angew. Chem.* **2001**, *109*, 1796; *Angew. Chem., Int. Ed.* **2001**, *40*, 2073.
(25) Abashkin, Y. G.; Collins, J. R.; Burt, S. K. *Inorg. Chem.* **2001**, *40*, 4040.
(26) Cavallo, L.; Jacobsen, H. *Eur. J. Inorg. Chem.* **2003**, 892.
(27) Khavrutskii, I. V.; Musaev, D. G.; Morokuma, K. *Inorg. Chem.* **2003**, *42*, 2606.
(28) Cavallo, L.; Jacobsen, H. *J. Phys. Chem. A* **2003**, *107*, 5466.
(29) Cavallo, L.; Jacobsen, H. *J. Org. Chem.* **2003**, *68*, 6207.
(30) Feichtinger, D.; Plattner, D. A. *Angew. Chem.* **1997**, *109*, 1796; *Angew. Chem., Int. Ed. Engl.* **1997**, *36*, 1718.
(31) Linker, T. *Angew. Chem.* **1997**, *109*, 2150; *Angew. Chem., Int. Ed. Engl.* **1997**, *36*, 2060.
(32) Brandt, P.; Norrby, P.-O.; Daly, A. M.; Gilheany, D. G. *Chem. Eur. J.* **2002**, *8*, 4299.

picture that emerged from the early studies needs to be broadened, due to the fact that a radical intermediate was located for cationic systems as well.[26]

Enantioselective, as well as catalytic, aspects of the Jacobsen−Katsuki epoxidation are not considered in Figure 1. While the first aspect has been given computational attention,[23,33] it is noted that questions dealing with the generation and regeneration of the catalytically active species have not yet been addressed.

In view of these previous computational studies, and referring back to the early reports of hypochlorite as effective oxidant, we advance a different explanation for the Mn−salen catalyzed epoxidation of olefins, based on the catalytically active species **3** (Chart 3).

Chart 3

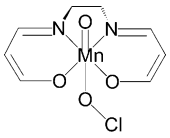

3

In the present work, we will illustrate that a reaction scheme based on complex **3** not only allows us to rationalize a spin-conserving reaction path, but also holds potential evidence for a reaction sequence that incorporates regeneration of the catalyst, and thus closure of the catalytic cycle.

2. Computational Approach

Spin unrestricted, gradient corrected density functional calculations were carried out, with corrections for exchange and correlation according to Becke[34] and Perdew,[35] respectively (BP86). There has been a recent discussion in the literature as to whether pure or hybrid density functionals provide the most appropriate computational vehicle for this kind of calculation.[25,27] We could show that the popular functionals BP86 and B3LYP provide not only quantitatively different but also qualitatively different descriptions,[28] and that the interpretation of the computational results therefore should be approached with care. In view of a recent study comparing high-level *ab initio* results obtained from coupled-cluster calculations with different DF approaches, it appears that BP86 might represent the more appropriate choice of functional for this type of calculations.[25] Furthermore, we have performed additional B3LYP single point calculations on optimized structures corresponding to local minima. In any case, no sign of net inversion of the relative stability between states of different multiplicity was observed.

Main group elements have been described by a split-valence basis set with polarization,[36] and Mn was treated with a valence triple-ζ basis set[37] plus one additional p-function ($\alpha = 0.12765$). Previous studies have already illustrated the importance of a fully polarized basis set, and of a triple-ζ, description of the transition metal center, when considering the relative energetic order of different spin states.[26,28]

We considered triplet as well as quintet states when describing the potential energy surface of the oxygen transfer step. Previous calculations have indicated that a singlet state is of some relevance in cationic, but not in neutral, model complexes.[26] Therefore, singlet states will only be considered for selected structures. Recently, Abashkin and Burt demonstrated that singlet states are only of importance when viewed in the context of a new reaction mechanism, which involves C−O bond formation between the substrate and an oxygen atom of the ligand system, a proposal that is not further considered in the present work.[51]

When talking about spin states in the framework of density functional theory, a caveat is in order. For an open shell system, with the exception of the highest spin state, it is generally not possible to exactly formulate a given spin state within density functional theory, and spin expectation values are normally constructed for an approximate wave function as Slater determinants from Kohn−Sham orbitals. To emphasize this point, we will exclude the terms triplet or quintet state for an electronic configuration based on electron densities, and in our nomenclature we will refer to S0, S2, and S4 systems, characterized by a total spin density of zero, two, and four unpaired electrons, respectively.

The model catalyst investigated in the present work is based on a Mn−acacen′ complex. A comparison of Mn−salen with Mn−acacen′ compounds validates the use of the chosen model.[22,29] Ethylene was chosen as model for the olefin.

The calculations were performed utilizing the Gaussian98 program system.[38] Total free energies in solution including all nonelectrostatic terms (E_{sln}) were estimated by performing a single-point, self-consistent reaction field calculation for optimized in vacuo structures according to the polarizable continuum model (PCM).[39] For all calculations, a convergence criterion of 1.0×10^{-6} was adopted for changes in energy and density matrix elements.

Local minima on the potential energy surface were characterized by real frequencies only, while transition states were characterized by an imaginary frequency, corresponding to a molecular displacement along the reaction coordinate. For the numerical integration, a 75 radial shells and 302 angular points per shell pruned grid was employed, except for structures of precomplexes S2-**4** and S4-**4**,

(33) Norrby, P.-O.; Linde, C.; Åkermark, B. *J. Am. Chem. Soc.* **1995**, *117*, 11035.
(34) Becke, A. D. *Phys. Rev.* **1988**, *A38*, 3098.
(35) Perdew, J. P. *Phys. Rev.* **1986**, *B33*, 8822.
(36) Schäfer, A.; Horn, H.; Ahlrichs, R. *J. Chem. Phys.* **1992**, *97*, 2571.
(37) Schäfer, A.; Huber, C.; Ahlrichs, R. *J. Chem. Phys.* **1994**, *100*, 5829.
(38) Frisch, M. J.; Trucks, G. W.; Schlegel, H. B.; Scuseria, G. E.; Robb, M. A.; Cheeseman, J. R.; Zakrzewski, V. G.; Montgomery, J. A., Jr.; Stratmann, R. E.; Burant, J. C.; Dapprich, S.; Millam, J. M.; Daniels, A. D.; Kudin, K. N.; Strain, M. C.; Farkas, O.; Tomasi, J.; Barone, V.; Cossi, M.; Cammi, R.; Mennucci, B.; Pomelli, C.; Adamo, C.; Clifford, S.; Ochterski, J.; Petersson, G. A.; Ayala, P. Y.; Cui, Q.; Morokuma, K.; Malick, D. K.; Rabuck, A. D.; Raghavachari, K.; Foresman, J. B.; Cioslowski, J.; Ortiz, J. V.; Stefanov, B. B.; Liu, G.; Liashenko, A.; Piskorz, P.; Komaromi, I.; Gomperts, R.; Martin, R. L.; Fox, D. J.; Keith, T.; Al-Laham, M. A.; Peng, C. Y.; Nanayakkara, A.; Gonzalez, C.; Challacombe, M.; Gill, P. M. W.; Johnson, B. G.; Chen, W.; Wong, M. W.; Andres, J. L.; Head-Gordon, M.; Replogle, E. S.; Pople, J. A. *Gaussian 98*, revision A.5; Gaussian, Inc.: Pittsburgh, PA, 1998.
(39) Miertus, S.; Scrocco, E.; Tomasi, J. *Chem. Phys.* **1981**, *55*, 117.
(40) Boys, S. F.; Bernardi, F. *Mol. Phys.* **1970**, *19*, 553; **2002**, *100*, 65.
(41) Desiraju, G. R. *Acc. Chem. Res.* **1991**, *24*, 290.
(42) Desiraju, G. R. *Acc. Chem. Res.* **1996**, *29*, 441.
(43) Whitesides, G. M.; Simanek, E. E.; Mathias, J. P.; Seto, T. C.; Chin, D. N.; Mammen, M.; Gordon, D. M. *Acc. Chem. Res.* **1995**, *28*, 37.
(44) Novoa, J. J.; Sosa, C. *J. Phys. Chem.* **1995**, *99*, 15837.
(45) Margl, P.; Deng, L.; Ziegler, T. *Organometallics* **1998**, *17*, 933.
(46) Palucki, M.; Pospisil, P. J.; Zhang, W.; Jacobsen, E. N. *J. Am. Chem. Soc.* **1994**, *116*, 9333.
(47) Cambell, K. A.; Lashley, M. A.; Wyatt, J. K.; Nantz, M. H.; Britt, R. D. *J. Am. Chem. Soc.* **2001**, *123*, 5710.
(48) Adam, W.; Roschmann, K. J., Saha-Möller, C. R. *Eur. J. Org. Chem.* **2000**, 3519.
(49) Adam W.; Mock-Knoblauch C.; Saha-Möller, C. R.; Herderich, M. *J. Am. Chem. Soc.* **2000**, *122*, 9685.
(50) Feichtinger, D.; Plattner, D A. *J. Chem. Soc., Perkin Trans. 2* **2000**, 1023.
(51) Abashkin, Y. G.; Burt, S. K. *Org. Lett.* **2004**, *6*, 59.

Scheme 2

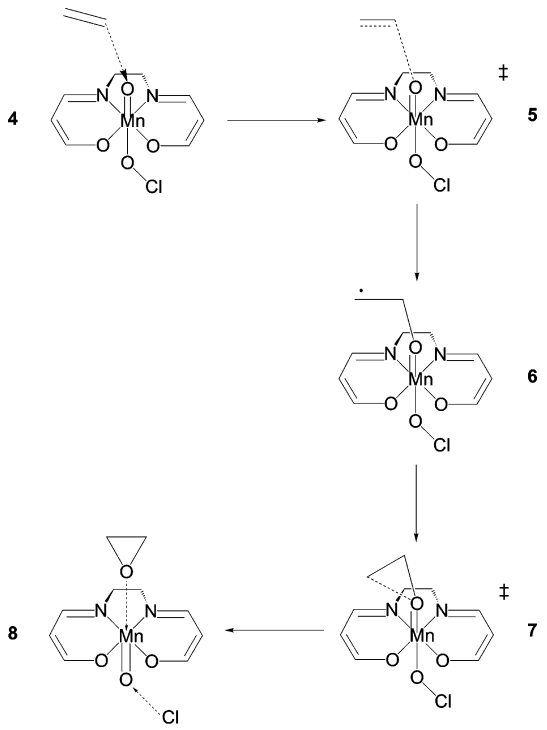

for which a pruned grid with 99 radial shells and 590 angular points per shell was used. This approach was also taken when optimizing the alternative coordination geometry for S2-**3**. Reaction energies involving a dissociation step have been corrected for basis set superposition errors (BSSE).[40]

3. Results and Discussion

Before engaging into a detailed discussion, a few remarks on the representation of the complexes considered are in order. Schematic representations of the relevant complexes are shown throughout the charts and schemes, and, as usual, are designated by bold numbers. When appropriate, these numbers are augmented by prescripts S2 and S4, referring to a complex having a total spin density of two and four electrons, respectively. Optimized geometries for all complexes considered are displayed in the Supporting Information and will assist the reader in following the arguments that are presented in the next sections.

3.1. The Catalyst and Oxygen Transfer. Oxygen transfer reaction sequences and corresponding energy profiles are based on a protocol put forth in previous mechanistic studies,[20,22] as shown in Scheme 2. The olefin approaches complex **3**, and forms the weakly bound precomplex **4**. This complex serves as zero energy reference state for the reaction profiles to be presented. A first transition state **5** for the first C−O bond-forming step leads to radical intermediate **6** while a second transition state **7** for the second bond-forming step furnishes the final epoxide.

The reaction sequence was investigated on the S2 as well as on the S4 surface, as mentioned above. The optimized geometry for complex S2-**3** is displayed in Figure 2.

Relevant Mn−O and Mn−N bond distances compare well with values reported[22] for the Mn−oxo complex S2-**3b**. Distances between the transition metal centers and the oxo-

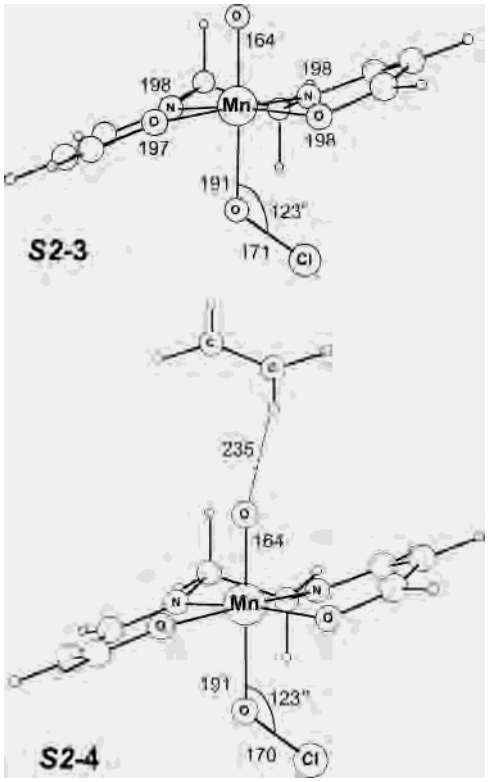

Figure 2. Optimized BP86 geometries for the oxo catalyst S**2-3** and the olefin precomplex S2-4.

ligands are virtually identical in complexes S2-**3** and S2-**3b**; Mn−O and Mn−N bond lengths defining the coordination geometry for the acacen′ ligand are slightly longer in S2-**3**, about 1−2 pm. As to be expected, the hypochlorite ligand is bonded to Mn at an angle ∠(Mn−O−Cl) close to 120°. Under coordination to the transition metal center, the O−Cl bond distance shortens by about 4 pm. Complex S2-**3** reveals the characteristic folded geometry of the acacen′ ligand system, with relevant folding angles[26] φ_+ and φ_- amounting to 156° and 165°, respectively. These values fall within the typical range of fold angles determined for a variety of neutral Mn−salen complexes.[29] As already reported in the literature, the folded geometry of the Schiff base ligand and formation of a chiral pocket is an essential element in enantioselective epoxidation.[23,33]

Complex S4-**3**, characterized by a significantly longer bond distance for the oxo ligand of 176 pm, is 71 kJ/mol higher in energy compared to S2-**3**. The folding angles φ_+ and φ_- for S4-**3** amount to 168° and 175°, approaching the value of 180° for a planar ligand system. In complex **3**, regardless of the spin density, the OCl^- ligand is bonded to the transition metal center via the oxygen atom. Alternative coordination geometries, in which the OCl^- ligand is bonded through Cl, have also been considered. On the S2 surface, a weakly bonded complex was found, displaying a Mn−Cl separation of 268 pm. This complex is 86 kJ/mol above S2-**3**. On the S4 surface, the geometry optimization resulted in a system in which the OCl^- is separated from the Mn−acacen′ complex by 291 pm. This system is 108 kJ/mol higher in energy, when compared to S2-**3**. It is concluded that this

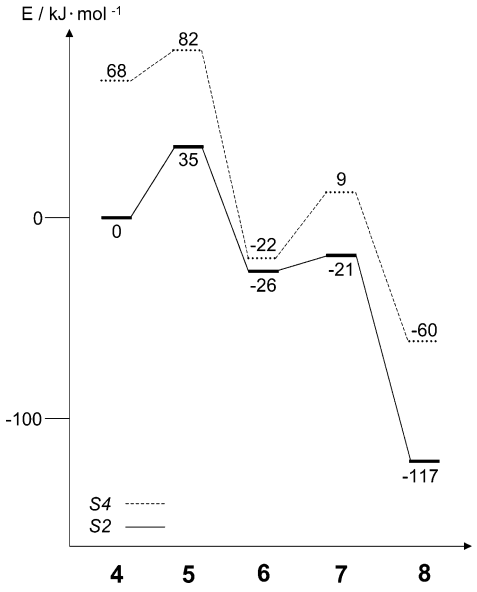

Figure 3. Reaction profiles for the oxygen transfer reaction on the S2 surface (—), and on the S4 surface (- - -). Along the axis of abscissae, **4** represents the precomplex, **5** the first transition state, **6** the radical intermediate, **7** the second transition state, and **8** the final product.

alternative coordination mode of the hypochlorite ligand deserves no further consideration.

Before turning to the energy profile associated with the reaction proposed in Scheme 2, we take a closer look at the precomplex geometry **4**. The optimized geometry for complex S2-**4** is also displayed in Figure 2. The incoming olefin approaches the oxo ligand and forms a C−H···O hydrogen bond. This type of hydrogen bonding is well established in the solid state, and its implication as structure defining principle as well as its application in crystal engineering have received a great deal of attention.[41,42] However, the C−H···O hydrogen bond also plays an important role in molecular recognition.[43] The performance of density functional calculations in characterizing such interactions has been systematically studied.[44] In view of these results, the BP86 approach together with a sufficiently large basis set can be expected to produce reasonably good data. The calculated bond length of 235 pm represents a typical value for such weakly bonded systems. For precomplex S4-**4**, a somewhat stronger bond is calculated, having a C−H···O bond length of 227 pm. It is this weak interaction that likely initiates the process of oxygen transfer, rather than an interaction between the π electron cloud of the olefin and the oxo ligand. Thus, the formation of a hydrogen bond might well have a significant influence on the directional approach of the olefin. However, the reader is reminded that the above discussion is intended to provide impetus for further investigation. The points raised merely reflect the property of the model system under investigation, and may or may not be of special importance for the real situation.

3.2 Energetic Considerations. Energy profiles for the oxygen transfer reactions on the S2 and S4 energy surfaces are displayed in Figure 3. The S2-energy profile for the reaction of S2-**3** with ethene closely resembles that of system S2-**3b** + C_2H_4,[22] and so do the molecular structures of the first transition state S2-**5** and the radical intermediate S2-**6**

Scheme 3

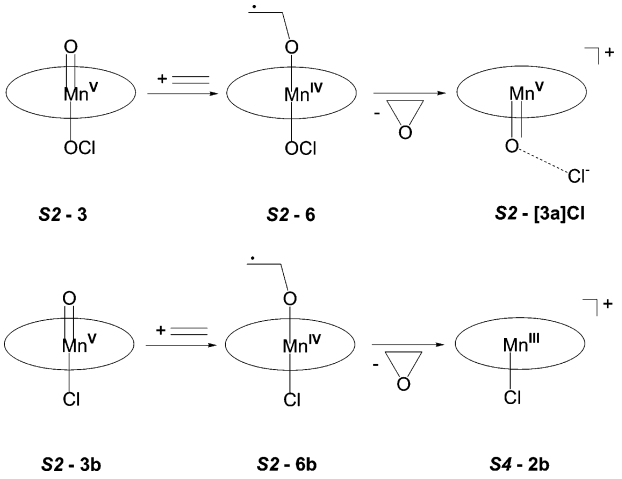

(compare Scheme 2). As an important difference, a significantly larger activation barrier of 35 kJ/mol for the first C−O bond formation is calculated for system S2-**3** + C_2H_4 (Figure 3), compared to the value of 12 kJ/mol for system S2-**3b** + C_2H_4.[22] Since the first bond formation step determines the enantioselectivity of the epoxidation reaction, a higher activation barrier might lead to enhanced chiral discrimination and higher enantiomeric excess. However, one has to keep in mind that an initial high enantiomeric excess might be lost if the life duration of the radical intermediate is long enough to allow racemising rotation around the newly formed C−O bond. The life span of the radical intermediate depends on the activation energy required for the formation of the second C−O bond. For both systems S2-**3** and S2-**3b**, the second bond formation step is calculated to require only a small activation barrier of 5 and 4 kJ/mol, respectively (compare Figure 3 and ref 22). An important distinction emerges between oxygen transfers originating from complex S2-**3** and complex S2-**3b** (Scheme 3).

In the catalytic system containing a hypochlorite ligand, the reaction initiates from a Mn(V) oxo complex S2-**3**, proceeds through a Mn(IV) radical intermediate S2-**6**, and terminates with the formation of an epoxide and another Mn(V) complex [S2-**3a**]Cl^-. The preferred spin state for all the transition metal complexes is an S2 state. On the other hand, starting from the Mn(V) compound S2-**3b**, the Mn(IV) radical intermediate S2-**6b** leads to formation of the Mn(III) complex S4-**2b**. Whereas the oxo compound and the radical intermediate display a preference for an electronic S2 state, the final five-coordinated compound clearly favors an electronic S4 state.[22] Thus, an oxygen transfer reaction originating from S2-**3** is likely to proceed as spin-conserving reaction, whereas the reaction profile originating from complex S2-**3b** suggests the possibility of intersystem spin crossing, the spin change driven by the existence of Mn(III) complex on the product side.

When discussing spin conserving reaction pathways, a brief discussion of possible singlet spin states is in order. For the Mn(V) oxo complexes, S0 states appear to be the electronically most stable states, but the S0 and S2 states are reported to be close in energy.[26] In the present work, we calculate the S0 preference for complexes **3** and **3b** to amount

to 4 and 3 kJ/mol, respectively. This finding is in accord with our previous results.[22,26] Further, we were able to show that, going from model systems with acacen′ ligands to systems with salen ligands, the energetic preference for the S0 state is lifted, due to possible electron delocalization onto the aromatic subsystem of the salen ligand.[29] Therefore, we propose that the S2 model system presents a realistic approach to the actual systems used in the laboratory.

We now turn to the energy profile on the S4 surface (Figure 3). The first reaction sequence S4-**4** → S4-**5** → S4-**6** again resembles that of system S4-**3b** + C_2H_4. In both cases, the S4 precomplex is significantly higher in energy than the corresponding S2 precomplex. Further, in both cases, the S2 and S4 radical intermediates are close in energy, the S2 system being favored over the S4 system by 4 kJ/mol (compare Figure 3) and 9 kJ/mol[22] for systems with hypochlorite and chloride counter ligands, respectively. Significant differences, however, occur in the second reaction sequence S4-**6** → S4-**7** → S4-**8**. In the system derived from complex S4-**3**, the second C−O bond formation on the S4 energy surface requires an activation energy of 31 kJ/mol, which is about 2.5 times the value calculated for the system derived from S4-**3b**. Also, complex S4-**8** is 62 kJ/mol higher in energy than compound S2-**8**, and the energy profiles, as shown in Figure 3, do not suggest that the a spin change is energetically favorable to any reaction step during oxygen transfer. The second transition state on the S4 surface is not energetically preferred over, or close in energy to, the one on the S2 surface, nor is the final product on the S4 surface more stable than the final product on the S2 surface. This is in contrast to the previously reported reaction profiles,[20,22] which hint at the possibility of spin change during the formation of the final product (compare Figure 1). An inspection of the S2-**8** and the S4-**8** geometries indicates that in both cases the product formation is accompanied by reoxidation of the metal center. Thus, the final products resemble the corresponding oxo complexes S2-**3** and S4-**3**, and display the same preference for an S2 state. This could very well explain a reaction occurring under conservation of spin. These observations, combined with the fact that structures and relative energies on the S2 and S4 energy hypersurfaces are not dramatically different, render unlikely that spin-change constitutes the major principle determining enantioselectivity of the Jacobsen−Katsuki epoxidation.

3.3. The Final Step in Product Formation. Figure 4 displays geometries for the transition state **7** on the S2 and S4 surfaces. Complex S2-**7** is characterized by a long C−O separation of the newly forming bond by 211 pm. Compared to complex S2-**4**, the Mn−O bond for the oxo ligand is elongated by 26 pm, indicating the step of dissociation of the forming epoxide molecule. At the same time, the bond length of the hypochlorite ligand begins to shorten. In contrast, the transition state bond length of the forming C−O bond is significantly shorter for structure S4-**7**. Whereas the transition state on the S2 surface might be characterized as an early transition state, the corresponding local maximum on the S4 surface might be interpreted as a late transition state. This observation provides an explanation for the difference in activation energy of 30 kJ/mol in favor of the

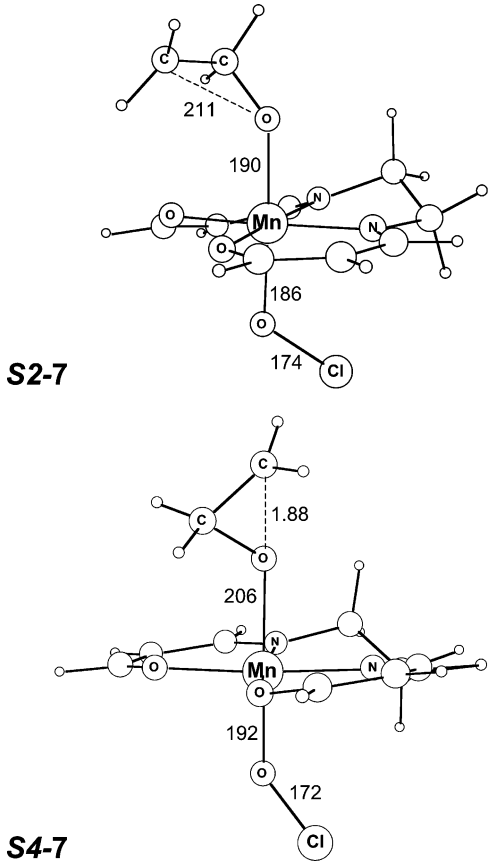

Figure 4. Optimized transition states for the second C−O bond formation on the S2 and S4 surfaces.

S2 profile. This value is obtained when comparing the relative energies of complexes S2-**7** and S4-**7** (compare Figure 3).

The last step of the reaction profile, the formation of the final product from the second transition state, has been further investigated by an intrinsic reaction coordinate (IRC) analysis. Starting from the second transition state S2-**7**, the product formation has been traced in order to validate the important characteristics of the reaction as outlined above. Changes in important geometric parameters along the intrinsic reaction coordinate *s* are plotted in Figure 5, and during the reaction, the values of *s* ranges from 0.00 amu$^{1/2}$·b to 5.50 amu$^{1/2}$·b.

The formation of the epoxide is traced in Figure 5a. Here we observe a steady decrease of the relevant C−O separation, which indicates bond formation, accompanied by a lowering of the total energy *E*. At $s = 3.75$ amu$^{1/2}$·b, the formation of the new C−O is complete, and the C−O bond length stays essentially constant during the last part of the reaction. The energy *E*, which up to this point has dropped by 87 kJ/mol, is still decreasing, but less drastically so, to reach the final value of 97 kJ/mol. During the course of the reaction, the Mn−O bond length increases steadily, indicating dissociation of the forming epoxide.

In Figure 5b, changes involving the hypochlorite ligand are monitored: the Cl−O bond distance extends, an effect that at $s = 3.75$ amu$^{1/2}$·b becomes more pronounced, and concurrently, the Mn−O bond length decreases steadily, an indication of reoxidation of the transition metal center.

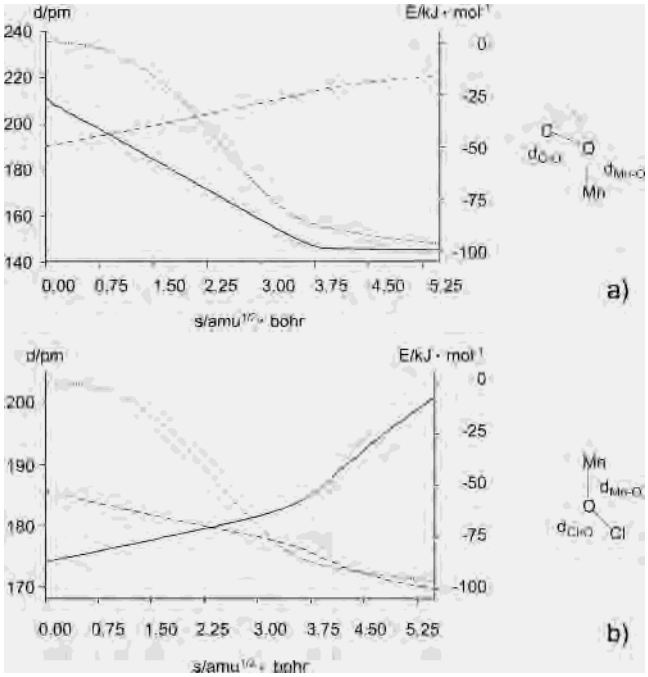

Figure 5. IRC traces of relevant geometric parameters relating to formation of the final product from the second transition state on the *S2* surface, followed by C−O (—) and Mn−O (- - -) distances of the forming epoxide (a), as well as Cl−O (—) and Mn−O (- - -) distances of the hypochlorite ligand causing reoxidation of the metal center (b). Also displayed is the accompanying change in energy (···).

From the results of Figure 5, it appears that the reaction initiated from transition state S2-**7** is to be described as a two-step process. The first part of the reaction path, 0.00 amu$^{1/2}$•b ≤ *s* ≤ 3.75 amu$^{1/2}$•b, is governed by C−O formation, whereas over the second part of the reaction, 3.75 amu$^{1/2}$•b ≤ *s* ≤ 5.50 amu$^{1/2}$•b, Cl^- dissociation is the characterizing feature. These changes are accompanied by processes of epoxide dissociation as well as oxo ligand formation. The IRC analysis reaffirms the conclusions that were drawn above. We then arrive at a final product *S2*-8, with bond distances of the oxo, epoxide, and chloride ligands of 170, 221, and 201 pm, respectively. However, caution is needed so as not to stretch the interpretation of the results obtained from the static calculations presented in this work beyond their limits. Solvent effects as well as entropy contributions may well be the factors causing the forming adduct to dissociate into the separate molecules and ions.

3.4. A Proposal for a Closed Catalytic Cycle. The conclusions obtained so far are summarized in the reaction scenario of Scheme 4, in which a catalytic cycle for the Mn−salen mediated alkene epoxidation is proposed. Our model is based on a biphasic reaction protocol, according to which a solution of alkene and catalyst in dichloromethane is combined with an aqueous hypochlorite solution in the form of common household bleach.[4]

The reaction sequence as shown in Scheme 4 is broken down into six different steps. Product formation (step III) and regeneration of the catalyst (step VI) provide the major driving forces behind catalytic epoxidation. The reaction as illustrated in Scheme 4 is favorable in terms of ΔE_{sln} (ΔE_{sln} being ΔE in solution; compare Section 2) as it renders the product formation thermodynamically preferred.

The reaction sequence begins with phase transfer of the catalyst into the organic phase, step I, for which a change in energy of −8 kJ/mol is estimated. Calculations on real catalytic precursors with salen and substituted salen ligands confirm the notion that phase transfer is not an energetically demanding process, and suggest the existence of a catalyst distribution equilibrium between the aqueous and the organic phase. Further, the equilibrium distribution is governed by the substituents of the salen ligand, which underlines the importance of a built-in phase transfer capability in the catalytic precursor.[18,19]

Scheme 4

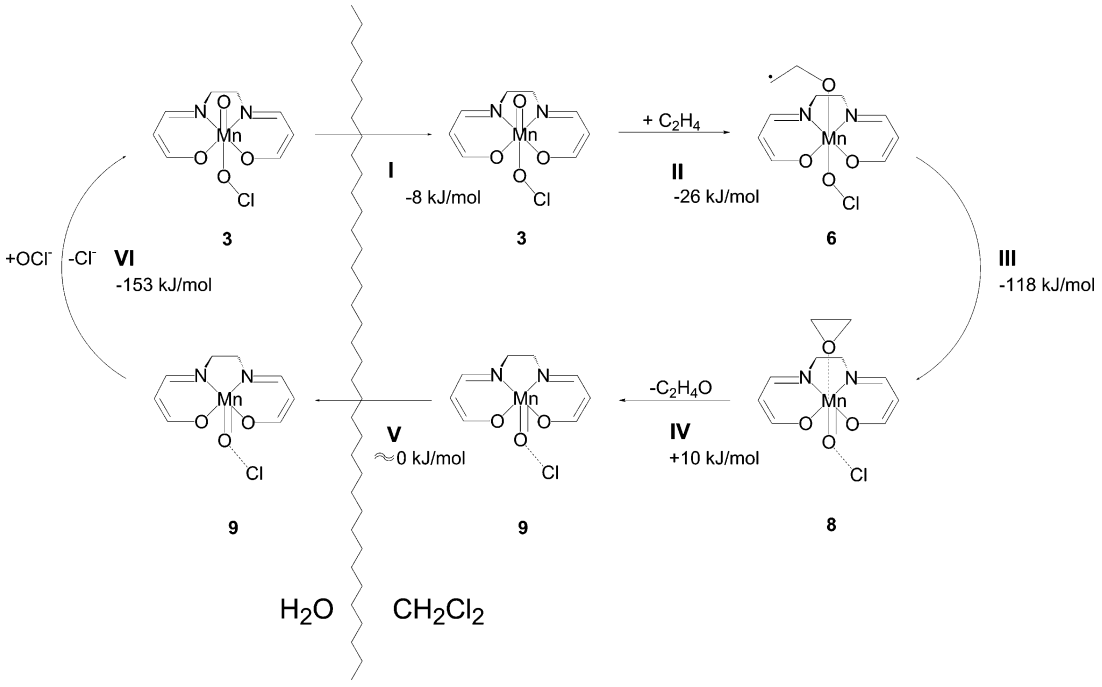

Taking place in steps II, III, and IV are the formation of the epoxide via a radical intermediate and the liberation of the final product. The corresponding ΔE_{sln} values amount to −26, −118, and +10 kJ/mol, respectively. Whereas the first two steps are energetically favored, the third step reflects the weak association energy of epoxide attachment to the transition metal center. When estimating an entropic contribution[45] $-T\Delta S$ in the range 40−50 kJ/mol at room temperature for step IV, it is reasonable to assume that product liberation is also favorable in terms of change in free enthalpy. Step VI leads to the formation of complex S2-**9**, in which a chloride ion is located in the coordination sphere of the cationic metal complex S2-**3a**.

In step V, a phase transfer occurs, in which the transition metal complex migrates into the aqueous phase, and in step VI, the catalyst is regenerated by a ligand exchange reaction. The last step is energetically favored, $\Delta E_{sln} = -153$ kJ/mol, and closes the proposed catalytic cycle.

On the basis of the above proposal, we can assign relevance to the role of additives in the Jacobsen−Katsuki epoxidation. *N*-Oxides such as *N*-methylmorpholine-*N*-oxide and 4-phenlypyridine-*N*-oxide lead to an enhanced enantioselectivity of the reaction.[46] Although originally thought to be a bond to the metal after the rate-limiting generation of the reactive Mn−oxo complex,[46] a recent dual-mode EPR study[47] revealed that additive formation takes place before oxygen transfer occurs. Experimental work demonstrates the importance of coordinating counterions in the enantioselectivity the reaction,[48,49] and our previous studies have shown that six-coordinated Mn−salen oxo species are inherently folded.[22,29] From a detailed computational study, it was concluded that additional ligands, which provide sufficient steric bulk, significantly influence the coordination geometry of the salen ligand by increasing its fold angle,[24] and thus assist in the generation of a chiral pocket. Such a chiral pocket was demonstrated to be a key element in determining the enantioselectivity of the epoxidation reaction.[23,33] After oxygen transfer, the organic nitrogen base is liberated and reoxidized by the oxygen donors present.

Not addressed in the above scheme are dimeric, binuclear complexes. Their presence and their role as reservoir species has recently been investigated by electrospray ionization in combination with tandem mass spectrometric techniques.[50] Although formation of a dinuclear cluster in direct correlation with epoxide formation has also been established by dual-mode EPR spectroscopy,[47] it seems reasonable to assume that such species are not directly involved in oxygen transfer to the olefinic double bond.

We are aware that the proposed reaction scheme does not hold definitive answers for all the problems related to the Mn−salen mediated alkene epoxidation. Other phase transfer processes might be envisioned, and the weak adducts **8** and **9** are likely to dissociate before the step of catalyst regeneration. Open questions not addressed in detail relate to the mechanism of ligand exchange in the initial formation of the catalytically active oxo species **3**. Nevertheless, the proposed model allows one to rationalize a spin conserving reaction pathway, and ties in with the experimental and theoretical insights gained in connection with the efficiency and selectivity of the Jacobsen-Katsuki reaction.

4. Conclusion

The scheme for the Jacobsen−Katsuki epoxidation that is proposed in the present work tentatively addresses the open questions related to its reaction mechanism. The presence of an oxygen containing counter ligand, such as hypochlorite, in *trans* position to the oxo group actively involved in the oxygen transfer process allows one to rationalize a reaction mechanism without the necessity to employ a spin crossing step. It further renders unlikely the possibility that spin-change be responsible for the enantioselectivity of the reaction. It further allows one to explain the regeneration of the active catalyst, and the closure of the catalytic cycle. The importance of counter ligands in promoting the oxidation reaction ties in with their role in determining the ligand geometry of the active catalyst. This in turn provides an intimate connection between catalytic and enantioselective aspects of the Mn-mediated alkene epoxidation. The results presented here provide therefore important insights in developing a unified picture of the Jacobsen−Katsuki epoxidation, and in establishing a catalytic scenario, which enables one to rationalize all characteristic aspects associated therewith.

Acknowledgment. The authors are indebted to CIMCF of the University "Federico II" of Napoli for technical assistance, and to Prof. T. K. Woo at University of Western Ontario and the SHARCNET project for generous access to computer resources. The authors further wish to thank Prof. M. Cossi and Dr. G. Scalmani of the University "Federico II" of Napoli for their invaluable assistance with the PCM calculations.

Supporting Information Available: Listing of Cartesian coordinates and final energies for all optimized geometries, spin expectation values for open-shell systems, imaginary frequencies for transition states, as well as structures of optimized complexes. This material is available free of charge via the Internet at http://pubs.acs.org.

IC0353615